CHARACTERIZATION OF SOME HIGH ALUMINA REFRACTORY RAW MATERIALS

A.B.C. Dodson, D.Phil
Department of Physics, UST, Kumasi

ABSTRACT

The physical, thermal and mechanical properties of some clay and non-clay raw materials usually used for the manufacture of high alumina refractory bricks have been determined. The effects of coarse and fine grain sizes on the physical and mechanical properties were also investigated. The clay materials (Yakusa Kibushi clay, elutriated plastic clay and hard shale clay) exhibited large shrinkages (17-30%) and large weight losses (14-19%). The calcined clay or grog, on the other hand, had small volume shrinkages (up to 8%) and weight losses (up to 7%). The porosity of bricks prepared from a mixture of coarse (0.297-3.36 mm) and fine (under 0.297 mm) grains was on the average 27% lower than that made of only fine grains. Bulk densities of coarse-and-fine-grained clay bricks were larger than the corresponding values for the fine-grained bricks. The values for cold crushing strength were observed to be dependent on the bulk density, apparent porosity, the alumina content and the grain size distribution of the raw materials. The refractoriness of the raw materials increased with the alumina content.

KEY WORDS : *Refractory, porosity, abrasion, cold crushing strength, refractoriness, diffractogram, apparent density, bulk density, volume shrinkage.*

INTRODUCTION

There is a large number of different refractories which are made of alumina, silica, magnesia or chrome bearing ores. For example, the raw materials for a high alumina brick will consist of bauxite, sillimanite, alumina, some clay (to improve binding) and audalusite. The raw materials are blended in different proportions to achieve a particular set of properties for the bricks e.g. for high refractoriness and spalling resistance the alumina content should be high, and for high slag resistance alumino-silicate bricks are impregnated with chromium oxide [1].

Chemical analysis is performed to determine the different types of oxides and the relative amounts in the ores. X-ray diffraction analysis is used to analyze the crystalline phases present in raw materials. Other properties such as refractoriness, refractoriness under load, porosity, cold crushing strength may also have to be established. The characterization enables the brick maker to select the raw materials and to determine in which proportions they should be mixed. Different firing temperatures are also experimented with. After the brick had been fired further tests are then performed to arrive at the final set of properties. A short description of some of the raw materials will now be presented.

Clay Materials

Clay minerals are fine-particle-size hydrous aluminosilicates which show plasticity when mixed with water. Their chemical, physical and mineralogical characteristics [2,3] vary over a broad range. They are basically a layered structure which move readily over each other, giving rise to its physical properties of softness, swampy feel and easy cleavage. These physical properties make it possible for clay to be moulded into complex shapes. Clay minerals are classified into several groups according to their crystallographic structure:

a) Kaolinite group - $Al_2(Si_2O_5)(OH)_4$
b) Montmorillonite group-$Al_{1.67}Na_{0.33}(Si_2O_8)(OH)_2$
c) Micaceous group - $Al_4K_2(Si_6Al_2)O_{20}(OH)_4$
d) Aluminous group - AlOOH

Remarkable progress has been made in our understanding of clays over the past twenty years. Improvements in instrumentation have facilitated research into the structures and the interrelationships of the kaolin group of minerals [3] by X-rays, infra-red spectroscopy, electron microscopy and thermal methods. For example, X-ray diffraction and infrared spectroscopy have been used for identifying and quantifying disorders in kaolinite, and Mossbauer spectroscopy has furnished direct evidence for the substitution of aluminium by iron in kaolinite.

Natural occurring kaolinite abounds in many parts of the world, but for some special properties scientists have been able to develop synthetic kaolinite by adding water soluble ions or organic matter to compounds of alumina and silica. The product is highly white after sintering due to the low content of iron and titanium [4].

On heating kaolin up to 500°C the water of hydration is driven off and a meta-kaolin (an amorphous material) is formed. At 1100°C the free quartz in siliceous clay is converted to cristobalite. On further heating, the meta-kaolin is transformed to cubic spinel type structure by orderly recrystallization. The spinel type phase then decomposes into mullite and cristobalite

A.B.C. Dodson

with some amorphous and glassy phase [2]. At 1400°C, the mullite attains a distinct crystal structure. The essential equation of the transformation is given below:

$$3(Al_2O_3.2SiO_2.2H_2O) \text{ ----> } 3Al_2O_3.2SiO_2 + 4SiO_2 + 6H_2O$$

Clay → Mullite; Cristobalite

The mullite crystals are oriented in relation to the original Kaolinite. At 1350°C the relative proportions of the phases are 30% mullite, 15% cristobalite and 55% glass [2]. The morphology of the mullite phase is needle-like. In fire clay bricks they are too small to be seen under the optical microscope but after slag attack or prolonged heating they become visible even to the naked eye.

Synthetic mullite powder has been produced from silica which has been obtained from rice hull and alumina, derived from a reaction between aqueous solution of ammonium sulphate and ammonia water [14].

Non-clay Materials

The above subject is discussed in connection with high alumina bricks. Some of the raw materials used are audalusite (orthorhombic), sillimanite (orthorhombic) and Kaynite (triclinic). These raw materials are good sources of alumina and silica. They all have the same formula - $Al_2O_3.SiO_2$, but different crystal structures. The relative proportions of alumina and silica in each raw material depends on the geological rock formation they are associated with, and also on the depth of the mine. On heating, they change to mullite and glass or to mullite, glass and cristobalite [2,3].

This paper is on the characterization of some raw materials used in the manufacture of high alumina bricks. In a different paper to be published [6], the results on the properties of refractory bricks formed by blending some of the raw materials (mentioned here) have been discussed. The raw materials used were obtained from South Africa, China and South Korea. The method of investigation could be applied to any raw materials.

EXPERIMENTAL METHODS

Primary Preparation of Raw Materials

The primary preparation of the raw materials involved the crushing of the ores into smaller sizes by jaw crushers and grinding using a ball mill or a vibrating mill. The grains were then separated into different sizes by a vibrating screen and then stored away in different storage facilities for later use. The author was not involved in the primary preparation of the raw materials. Green body preparation started with the screened materials.

Green Body Preparation of Raw Materials

Two grain sizes of the raw materials were chosen, i.e. 0.297-3.36 mm (coarse grains) and 0.297 mm and under (fine grains). Different amounts of the raw materials with two different grain size distributions (Table 1) were weighed and placed in a mortar and thoroughly mixed with a pestle. Water was added to the clay materials, and dextrin to the non-clay materials. For each raw material, with the exception of elutriated plastic clay and Yakusa Kibushi (Ball) Clay, which were prepared with fine grains, the bricks were produced in sets of fine-grained and a blended coarse-and-fine-grained bricks. Table 1 shows the type of raw

Table 1. WEIGHT PERCENTAGES OF RAW MATERIALS USED FOR BRICKS

RAW MATERIALS	PERCENTAGE (%) WEIGHTS OF RAW MATERIALS FOR THE COARSE-AND-FINE-GRAINED BRICKS					
	PRYO	EPCC	HSCL	ANDA	MULL	HSCC
ELUTRIATED PLASTIC CLAY - POWDER (EPCL)	-	-	-	-	-	-
YAKUSA KIBUSHI (BALL) CLAY POWDER (YKCL)	-	-	-	-	-	-
HARD SHALE CLAY - COARSE GRAIN (HSCL)	-	-	40	-	-	-
HARD SHALE CLAY - POWDER (HSCL)	-	-	60	-	-	-
ANDALUSITE - COARSE GRAIN (ANDA)	-	-	-	40	-	-
ANDALUSITE - POWDER (ANDA)	-	-	-	60	-	-
SYNTHETIC MULLITE - COARSE GRAIN (ANDA)	-	-	-	-	40	-
SYNTHETIC MULLITE - POWDER (ANDA)	-	-	-	-	60	-
PYROPHYLLITE - COARSE GRAIN (PYRO)	40	-	-	-	-	-
PYROPHYLLITE - POWDER (PYRO)	60	-	-	-	-	-
ELUTRIATED PLASTIC CLAY (CHAMOTTE) - GRAIN COARSE (EPCC)	-	40	-	-	-	-
ELUTRIATED PLASTIC CLAY (CHAMOTTE) - POWDER (EPCC)	-	60	-	-	-	
HARD SHALE CLAY (CHAMOTTE) - COARSE GRAIN (HSCC)	-	-	-	-	-	40
HARD SHALE CLAY (CHAMOTTE) - POWDER (HSCC)	-	-	-	-		60

materials and the proportions used in the making of the bricks. Amounts of the mixture ranging from 310 to 570 gm were placed in a die in a forming machine and pressed to pressures between 34-98 MPa into green bodies (unfired) of dimension 60mm x 61mm x 61mm. The green bodies of the clay materials were produced in cylinders of dimension 60mm diameter x 61mm height. A set of five bodies were prepared for each raw material. The green bodies were dried in a pre-heated oven at 112°C for 2 days. The clay bodies were then fired at 1320°C and the non-clay bodies at 1450°C in a tunnel Kiln.

Volume Shrinkage and Weight Loss Measurements

The dimensions of the bricks were taken after forming, drying and firing. Weight losses were also recorded. Volume shrinkages were calculated as follows:

$$\left\{\begin{matrix}\%\ \text{Vol. Shrinkage of} \\ \text{rectangular brick}\end{matrix}\right\} =$$

$$[1-(1-\Delta w)(1-\Delta l)(1-\Delta h)] \times 100 \qquad (1)$$

$$\left\{\begin{matrix}\%\ \text{Vol. Shrinkage of} \\ \text{cylindrical brick}\end{matrix}\right\} =$$

$$[1-(1-\Delta d)^2(1-\Delta h)] \times 100 \qquad (2)$$

where

Δw - % change in width
Δh - % change in height
Δl - % change in length
Δd - % change in diameter

$$\%\ \text{Weight Loss} = \frac{m_i - m_f}{m_i} \times 100 \qquad (3)$$

where m_i and m_f are initial and final weights after drying or after firing.

Apparent Porosity, Apparent Density and Bulk Density of Fired Bricks

The Hot Test Piece, Boiling Water (HTBW) method was employed [2,5,7] for the measurement of apparent porosity, apparent and bulk densities. The bricks were inspected for any floss and cleared of any particles liable to detach and then weighed in air (W_1). The test pieces were kept in a pre-heated oven at 112°C for 24 hours to drive off any absorbed moisture. The test samples were then transferred quickly into a tank of boiling water. The boiling was continued for 3 hours, after which they were gradually cooled to the prevailing cold water temperature. The saturated bricks were weighed in air (W_2) and then in water (W_3). The apparent porosity, apparent density and bulk density were calculated as follows:

$$\text{Apparent porosity (\%)} = \frac{W_2 - W_1}{W_2 - W_3} \times 100 \qquad (4)$$

$$\text{Apparent density} = \frac{W_1}{W_1 - W_3} \times \text{density of water} \qquad (5)$$

$$\text{Bulk density} = \frac{W_1}{W_2 - W_3} \times \text{density of water} \qquad (6)$$

Chemical Analysis Using X-ray Fluorescence (XRF)

In X-ray fluorescence analysis the sample is irradiated with X-rays which induce secondary X-rays that are characteristic of the elements present in the sample. By measuring the wavelengths and the intensities of the secondary X-rays qualitative and quantitative analysis are performed on the samples [8-10]. A Rigaku X-ray spectrometer was used. Quantitative analysis can be performed on the basis that the intensity of the spectrum is proportional to the amount of the element present in the sample. Indirect method of determining oxide composition was employed. Standard samples with known oxide amounts were used to establish calibration curves of X-ray intensities against composition. These calibration curves were then used to determine oxide compositions in the raw materials.

X-ray Diffraction Analysis (XRD)

X-ray diffraction analysis [11] was performed for both the unfired and the fired raw materials. About 100 gm of each sample was placed in a vibrating mill to produce a powder, and 10 gm of it was passed through 297 μm sieve after quartering. XRD provides information on the types of crystalline phases present in the raw materials. A Rigaku diffractometer was used in the analysis. An aluminium plate with a square hole was placed horizontally on a table and the powder sample was pressed into it. The plate was then inserted in the sample holder in the machine. A monochromatic beam of X-rays (CuKα) was directed at the sample, and a computer controlled detector scanned from 10° to 60°, picking up the diffracted spectra. A chart recorder displayed the peaks. The Powder Diffraction Data File and the FINK index were used to identify the peaks.

Cold Crushing Strength (C.C.S.)

The bricks were sandwiched by cardboards and oriented such that the faces normal to the forming direction bore the axial load. The loads were applied by a compressive machine at the rate of 10 - 15kgf/cm²/sec until the test piece failed. The maximum load

TABLE 2: CHEMICAL COMPOSITIONS OF THE REFRACTORY RAW MATERAILS

RAW MATERIALS	L.O.I	SiO_2	Al_2O_3	Fe_2O_3	TiO_2	CaO	MgO	$Na_2O + K_2O$	MnO	TOTAL
ANDALUSITE	0.46	38.2	59.5	0.98	0.16	0.12	0.23	0.43	-	100.08
SYNTHETIC MULLITE	-	28.2	70.4	0.59	-	0.19	0.16	0.44	0.10	99.99
HARD SHALE CLAY (CHAMOTTE)	-	8.48	85.4	1.77	3.45	0.28	0.27	0.36	0.01	100.02
HARD SHALE CLAY	14.5	37.6	43.2	1.53	2.63	0.23	0.22	0.25	0.02	100.18
YAKUSA KIBUSHI (BALL) CLAY	10.1	56.5	27.6	2.58	1.06	0.20	0.48	1.56	0.02	100.10
PYROPHYLLITE	3.96	78.4	16.0	0.26	0.56	0.13	0.16	0.36	0.01	99.84
ELUTRIATED PLASTIC CLAY (CHAMOTTE)	-	60.9	32.4	2.59	0.77	0.21	0.49	2.49	0.03	99.88
ELUTRIATED PLASTIC CLAY	10.3	52.9	31.4	1.99	0.72	0.16	0.37	2.17	0.02	100.03

was recorded. The cold crushing strength (in MPa) was calculated as the ratio of the applied load to the cross sectional area of the brick normal to the load [5,12].

Refractoriness

The aim of this test was to compare the behaviour of a pyramidal test pieces with those of standard pyrometric cones of known seger cone numbers and express the refractoriness [5,13] as a cone number that approximates most closely to the behaviour of the test cone. Powder samples of the raw materials which had gone through mesh 50 (U.S.) were mixed with 2-3% dextrin and cast in a steel die. The cones were set in alumina sand together with some seger cones in a circular pattern. They were then dried at 104°C for 24 hours. Fig. 1 shows the standing positions of the test and standard cones. The cones were placed in a gas fired furnace raised to 2000°C at a rate of 10°C/min. The seger cone whose deformation most closely resembled that of the test cone when it bent properly and its top came in contact with the stand was assigned to the test cone. Temperatures were measured with an optical pyrometer.

RESULTS AND DISCUSSIONS

Chemical Analysis

The Oxide and impurity contents of the raw materials are shown in Table 2. The clays - Yakusa Kibushi and elutriated plastic had Al_2O_3 content of 27.6% and 31.4% respectively. Hard shale clay had 43.2% Al_2O_3. Calcined hard shale clay (Chamotte) increased dramatically in Al_2O_3 content, i.e. 85.4%.

The non-clay materials - audalusite and synthetic mullite had 59.5% and 70.4% Al_2O_3 respectively. Among

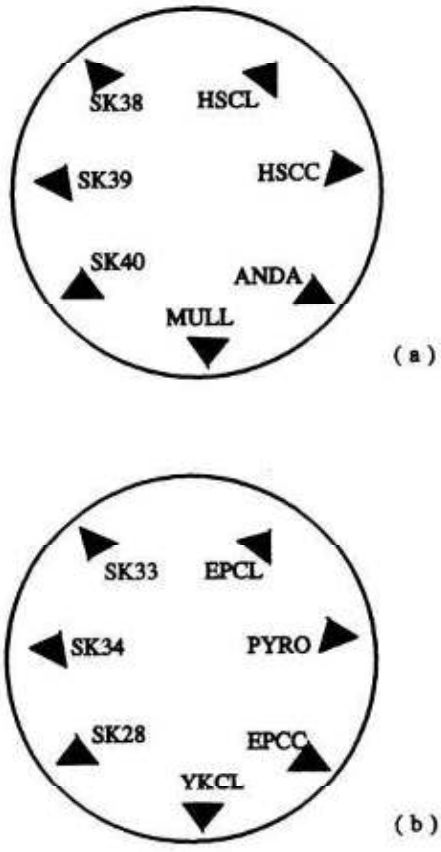

Fig 1. Arrangement of test and standard cones for refractoriness test.

the batch of raw materials considered, pyrophyllite had the highest amount of SiO_2 -78.4% and the lowest Al_2O_3 content - 16.0%. The loss of ignition (L.O.I.) was highest in the clays - hard shale clay (45%), Yakusa Kibushi (10.1%) and elutriated plastic clay (10.3%). Water and carbonaceous materials accounted for the ignition loss in the clays. The non-clay materials had low ignition losses of less than 0.5%. The loss of water and organic materials are always associated with large volume shrinkages and weight losses in clay materials as will soon be seen in the results on shrinkages.

X-Ray Diffraction Analysis of Unfired and Fired Raw Materials

The diffractograms are shown in pairs (Figs. 2-9) for the unfired and fired materials. Elutriated plastic clay (Fig.2), Yakusa Kibushi clay (Fig.3) and pyrophyllite (Fig.5) had some amount of free silica (quartz) which was converted to cristobalite during the firing. The amount of free silica in unfired pyrophyllite (Fig. 5a) was higher than those in unfired elutriated plastic clay (Fig.2a) and Yakusa Kibushi clay (Fig.3a). Fired pyrophyllite (Fig.5b) showed high peaks of quartz and low peaks of cristobalite. This implies that very little

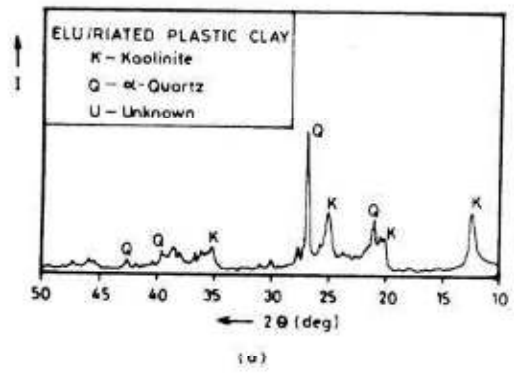

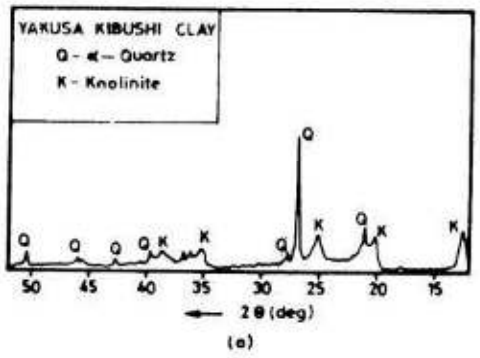

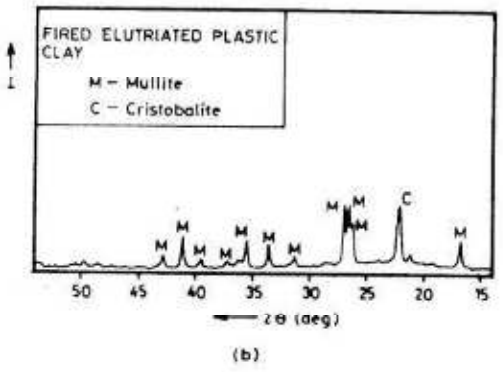

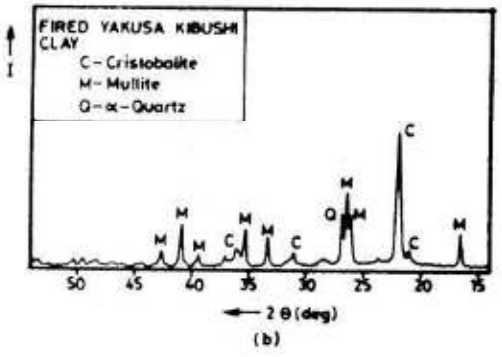

Fig 2. Diffractograms of unfired (a), and fired (b) elutriated plastic clay.

Fig 3. Diffractograms of unfired (a), and fired (b) Yakusa Kibushi clay.

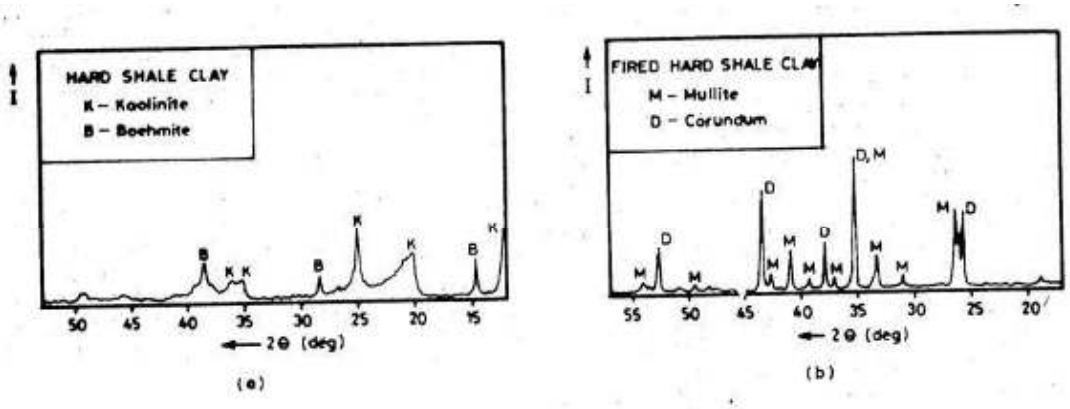

Fig 4. Diffractograms of unfired (a), and fired (b) hard shale clay.

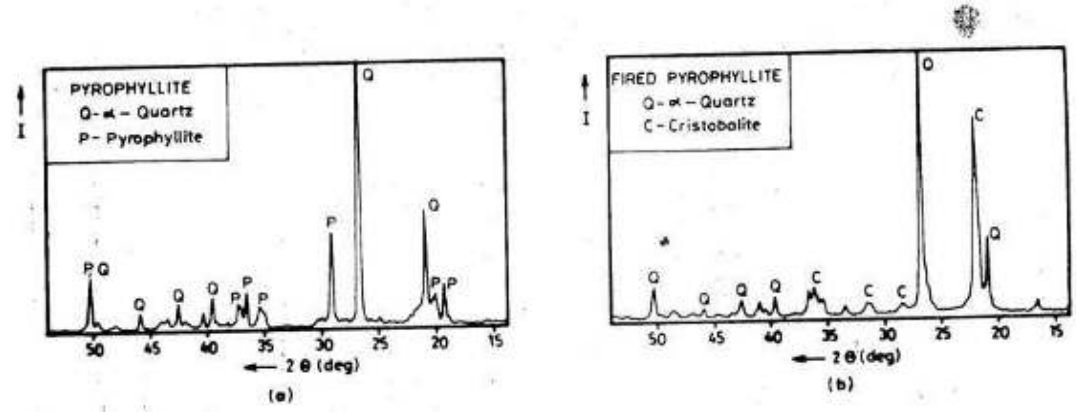

Fig 5. Diffractograms of unfired (a), and fired (b) pyrophyllite.

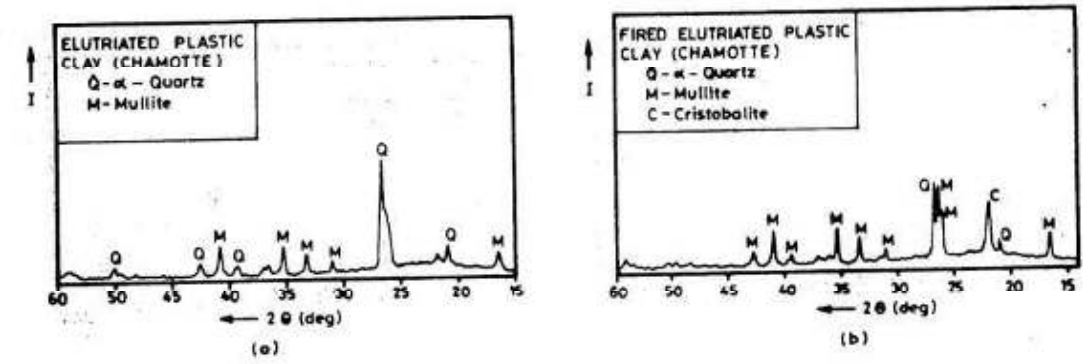

Fig 6. Diffractograms of unfired (a), and fired (b) elutriated plastic clay (chamotte)

of the quartz was converted into cristobalite. The firing period of 2 hours was also not long enough to cause a large portion of cristobalite to form. Such a high amount of quartz left after firing is detrimental to the performance of the brick as silica expands rapidly around 500°C [16]. Undue expansion in bricks could cause gaps between the bricks to be filled up, inducing internal stresses which could lead to spalling. The amount of quartz in elutriated plastic clay and Yakusa Kibushi clay was relatively low (Table 2) and therefore the firing temperature (1320°C) and period (2 hrs) were sufficient to convert all the quartz into cristobalite (Fig.2b, 3b). Kaolinite was identified in both elutriated plastic clay (Fig.2a) and Kibushi clay (Fig.3a).

The mullite transformation occurred in the clays after firing (Fig.2b, 3b). The mullite phase in alumino-silicate bricks is encouraged because of its excellent volume stability at temperatures up to 1850°C, and also because of its morphology of needle-like structures, capable of providing good strength. Unfired hard shale clay was found to consist of kaolinite and boehmite (bauxite) (Fig.4a). After firing, mullite and corundum (alumina) phases were formed (Fig.4b). It could be deduced from the relative heights of the mullite and corundum peaks (Fig.4b) that there was more conversion to alumina than to mullite.

When clay is pre-fired (before incorporation into refractories), it loses its plasticity and the material is called chamotte or grog. Several grades of alumino-silicate bricks have as a constituent some amount of chamotte to reduce shrinkage. The diffractograms of elutriated plastic clay chamotte and hard shale clay chamotte showed the mullite phase before and after firing.

For the non-clay materials, audalusite ($Al_2O_3.SiO_2$) after firing yielded sillimanite of the same chemical formula (Fig.8). The conversion to sillimanite was, however, not complete since there were some audalusite peaks (Fig.8b). There was no transformation after firing synthetic mullite (Fig.9a,b). This again showed the high thermal stability of mullite and hence its usefulness when added or induced in refractory bricks.

Volume Shrinkage and Weight Loss

The volume changes of the bricks after drying and firing are shown as bar charts in Fig. 10(a) & (b). The results of fine-grained bricks and coarse-and-fine-grained bricks are compared. Superimposed on the bar charts are line plots of weight losses after drying and

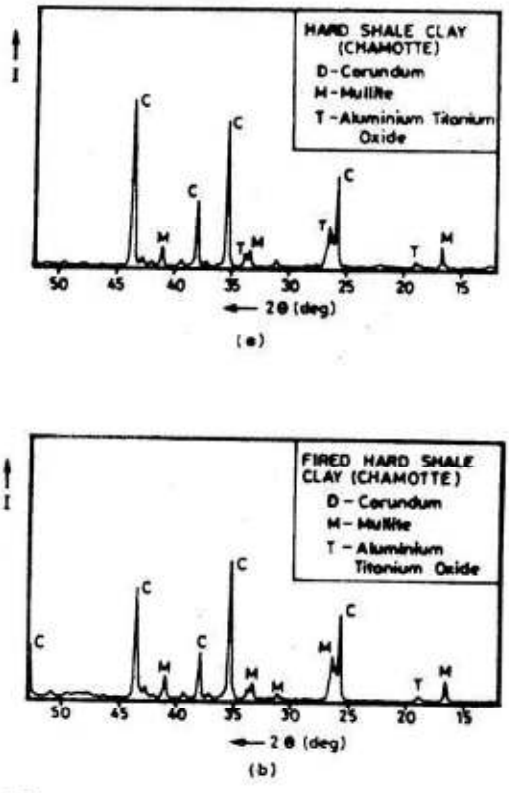

Fig 7. Diffractograms of unfired (a), fired (b) hard shale clay (chamotte)

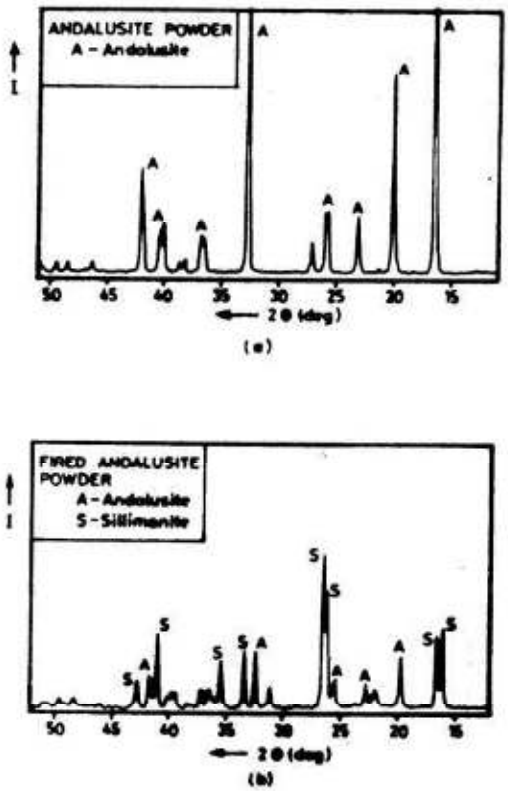

Fig 8. Diffractograms of unfired (a), fired (b) andalusite.

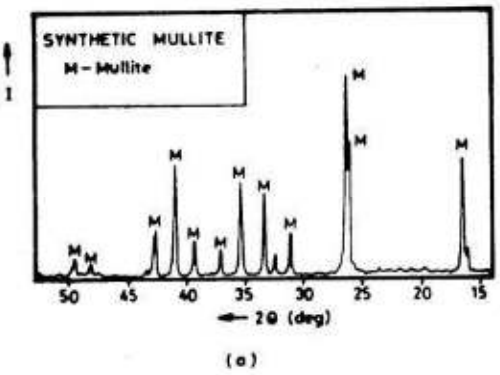

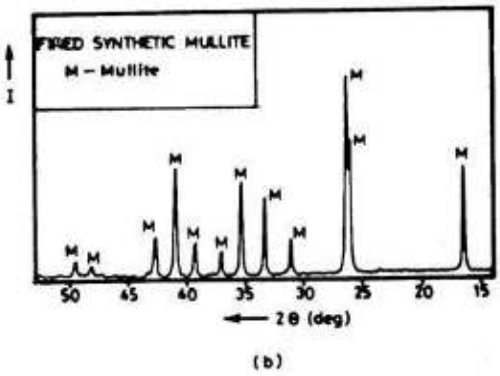

Fig 9. Diffractograms of unfired (a), fired (b) synthetic mullite.

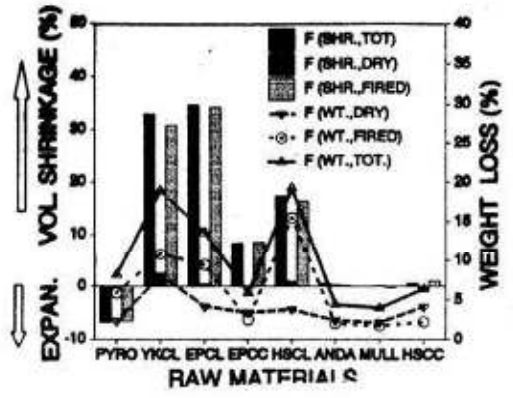

Fig 10a. A bar chart of percentage volume shrinkage and line plot of percentage weight loss for the fine-grained bricks.

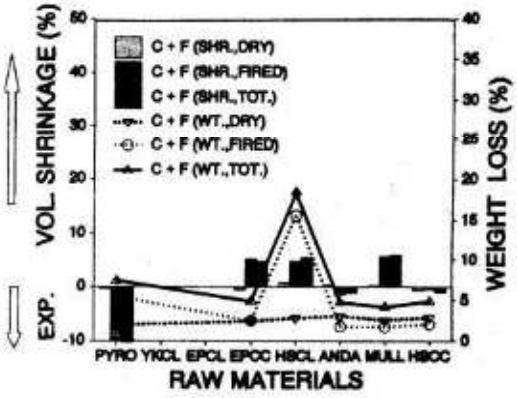

Fig 10b. A bar chart of percentage volume shrinkage and line plot of percentage weight loss for the coarse-and-fine-grained bricks.

firing. The fine-grained bricks of the clay materials (YKCL, EPCL and HSCL) went through 17-30% total volume shrinkage (drying and firing). Much of the shrinkage occurred after firing.

The complex structure of clay minerals is manifested even in their individual perculiarities of expansion and contraction behaviour. A number of clay minerals (e.g.China clay and halloysite) experience large contraction between 800 - 1000°C. The importance of knowing the shrinkage curves of the clay bodies lies not only in determining the fired size of the brick but also in adjusting the firing schedule to reduce the volume changes. Other factors that affect the shrinkage of a given body to a lesser extent are atmospheric conditions during firing, the grain size and deairing [5].

Apart from losses of water and organic material which resulted in shrinkage, the formation of glassy phase between the particles was also a shrinkage factor. The non-clay and chamotte bricks (ANDA, MULL, HSCC and EPCC) had much smaller volume shrinkages - less than 5%. The fine-grained brick of pyrophyllite exhibited a volume expansion of 10% after firing - this is attributed to the large amount of unconverted free silica in pyrophyllite (Fig.5a, b). The shrinkage

property of YKCL and EPCL bricks, and the expansion behaviour of PYRO bricks could be employed to control shrinkage in alumino-silicate bricks.

Pyrophyllite is a hydrous aluminium silicate ($Al_2O_3.4SiO_2.H_2O$) and hence chemically bears the same resemblance with clay minerals - it is not a clay material but plastic. It is crystalline and hence does not absorb ions or water. The main impurity in pyrophyllite is quartz - this makes the mineral abrasive in spite of the softness of pyrophyllite itself. The firing expansion of pyrophyllite in this work (i.e. 0 - 10%) is normal as pyrophyllite hardly shrinks at all on firing [5].

Percentage weight losses were found to be larger in the clay products than the non-clay bricks (Fig.10a).

The YKCL and the EPCL bricks were not included in the study of the coarse-and-fine-grained bricks because these raw materials were prepared only in the powder form. The PYRO coarse-and-fine-grained bricks once again showed an expansion 10% after firing. As a result of blending fine and coarse grains together the volume shrinkages of EPCC and HSCL bricks were reduced from 9% to 5%, and from 17% to 6% respectively (Fig.10a,b). The volume changes of the HSCC bricks switched from a volume reduction for fine-grained bricks to a volume expansion for coarse-and-fine-grained bricks. In both cases the volume change was less than 1%. It becomes clear from these findings that the shrinkage of bricks can be controlled by a number of measures, including the blending of coarse and fine-grained materials and by incorporating chamotte materials or grog [15]. The expansion of fired coarse-and-fine-grained bricks of ANDA bricks was slight, 1%. This expansion is attributed to the presence of sillimanite in the ANDA bricks (Fig.8b) [16]. For the corresponding fine-grained ANDA bricks there was a shrinkage of magnitude of 0.5%. The coarse-and-fine-grained MULL bricks showed a volume shrinkage of 6%. The degree of expansion of the bricks will usually depend on the relative amounts of the minerals present in the mixture.

Among the batch of coarse-and-fine-grained bricks the HSCL bricks had the highest value of percent weight loss - 17% (Fig. 10b). The PYRO bricks went through 7% weight loss and the non-clay bricks 5% or less. There was not much difference in the magnitude of percentage weight losses between the fine-grained and coarse-and-fine-grained bricks.

Apparent Porosity, Apparent Density and Bulk Density

The general trend of porosity results was that the coarse-and-fine-grained bricks had lower porosity than the fine-grained bricks (Fig.11). This trend was, however, reversed for only HSCL bricks. The decrease in porosity for coarse-and-fine-grained brick can be explained by considering the packing of coarse particles. The porosity of the assembly could further be decreased if smaller particles were added to fill spaces

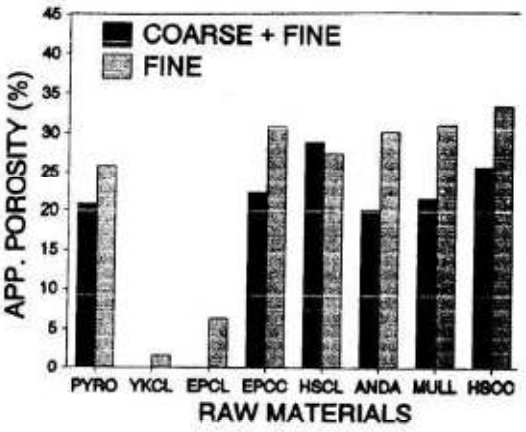

Fig 11. A bar chart of porosity of fine-grained and coarse-and- fine-grained bricks.

left by the coarse particles (Fig.12). The porosity of the aggregate brick would still be lower than that of only fine grains, for the reason that for a unit volume the aggregate would be more packed than the fine grains.

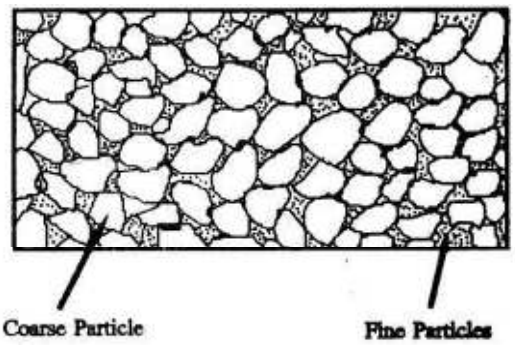

Fig 12. Aggregate of coarse and fine grains.

Low porosity has both advantages and disadvantages. In glass tanks and ladles for continuous casting, low porosity is required to reduce penetration of molten material and to slow down the rate of slag attack. A high porosity of 70% is not unusual for an insulation brick. The large volume of air pockets reduces the thermal conductivity of the brick and thus making it possible for the brick to retain heat in an enclosure i.e. furnace or Kiln.

The line plot for bulk and apparent densities are displayed in Fig.13 for fine-grained (F) and coarse-and-fine-grained bricks (C+F). It was observed that the apparent densities of the bricks were higher than their bulk densities - this is expected i.e.

$$\text{Bulk density} = \frac{\text{Dry Weight}}{\text{Volume of Brick}} \quad (7)$$

$$\text{Apparent density} = \frac{\text{Dry Weight}}{\text{Volume of Brick - Open Pore Volume}} \quad (8)$$

The denominator in equation (8) is smaller than that in equation (7), hence the apparent density will be larger. It was observed that for the non-clay bricks the bulk densities of the coarse-and-fine-grained bricks were larger than those of the fine-grained bricks. This means that for the same volume of brick, a coarse-and-fine-grained brick would have more materials packed into it than in a fine-grained brick. An increase in bulk density is therefore accompanied by a decrease in porosity. This is well illustrated for the non-clay materials- ANDA, MULL and the chamotte clays (EPCC and HSCC) in Fig.14. The YKCL and EPCL bricks did not have any coarse-and-fine-grained bricks and therefore no comparison could be made.

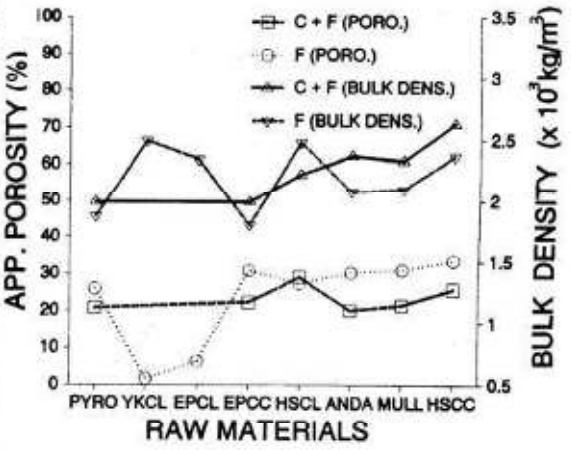

Fig 14. Line plots of apparent porosity and bulk density for fine-grained and coarse-and-fine-grained bricks.

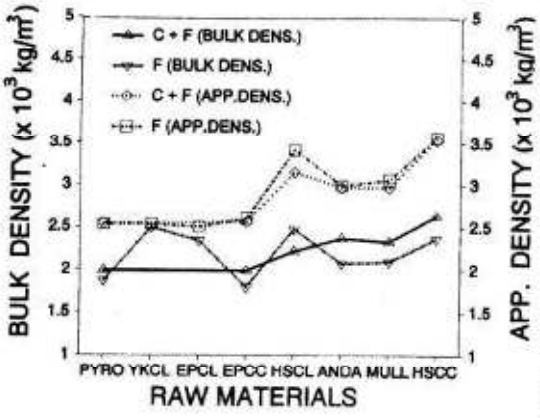

Fig 13. Line plots of apparent density and bulk density for fine-grained and coarse-and-fine-grained bricks.

Cold Crushing Strength (C.C.S.)

The values of cold crushing strength (C.C.S.) in Fig. 14 for some of the bricks i.e. ANDA, MULL and HSCC (Fig.15) were unusually high (80 - 100 MPa) as compared to the values for some commercial high alumina bricks (30 - 70 MPa). Raw materials are actually not used alone; a number of them are put together to achieve a desired set of properties. Cold crushing strength is, however, not the only property optimised in brick manufacturing. It is usually not a very important property at the service temperatures of the bricks. Refractoriness under load, for example, would be a more useful property to the brick user. However, C.C.S. values give some information on the degree of sintering during firing and the strength of the brick to withstand damage when being handled for export.

The general trend observed in Fig.15 was that fine-grained bricks had higher values of C.C.S. than the coarse-and-fine-grained bricks. This may be attributed to better sintering enhanced by the increase in surface area of fine particles. The ANDA and MULL bricks behaved differently i.e. the coarse-and-fine-grained bricks had higher C.C.S values than the fine-grained bricks. The hardness of the material is taken into consideration here. Andalusite grains are very hard i.e. 7 - 7.5 on the Mohs' scale (Diamond has 10).

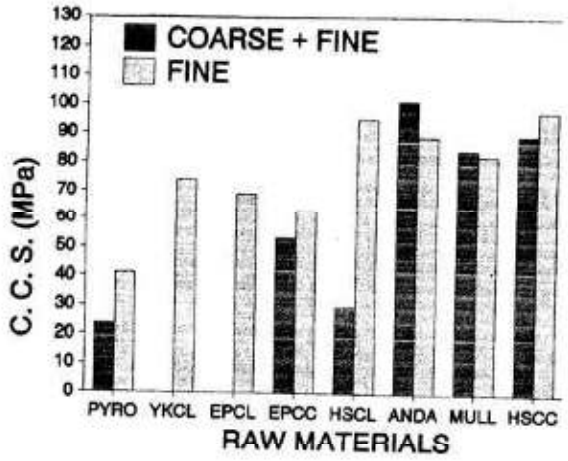

Fig 15. A bar chart of cold crushing strength (C.C.S.) for fine- grained and coarse-and-fine-grained bricks.

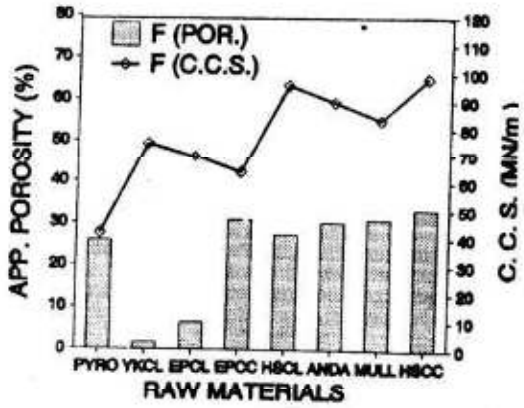

Fig 16b. A bar chart of apparent porosity and line plot of cold crushing strength (C.C.S.) for fine-grained bricks.

The hardness of mullite is not known but since it is made of about 72% of Al_2O_3 and the hardness of alumina (corundum) is 9 on the Mohs' scale, it is assumed that the hardness of mullite would be close to that of alumina. In view of the fore-going argument therefore, it would be expected that the grains of audalusite sintered with the fine particles would be able to support larger loads than the corresponding sintered fine grains only.

Figs. 16 (a),(b) show a fair correlation between C.C.S. and alumina content in the raw materials. There is a general increase of C.C.S. with alumina content for both categories of bricks. In Fig. 16b it is observed that the decrease in porosity from PYRO to YKCL is marked by a rise in C.C.S. value, but as the porosity increases from YKCL to EPCC, the C.C.S. values decrease. A similar behaviour is found for the HSCL, ANDA and MULL bricks (Fig. 16(a) & (b)). Increase in porosity reduces the effective amount of particle-to-particle contact in the brick, and hence its inability to support large loads, therefore low C.C.S values.

Some degree of correlation was also found between C.C.S. and bulk density in Figs 17 (a), (b). The correlation was well illustrated for the fine-grained bricks (Fig 17a). The broad maxima of bulk densities in going from PYRO to EPCC, and from EPCC to MULL are reflected in broad maxima of C.C.S. values. The C.C.S. values are therefore dependent of a number of

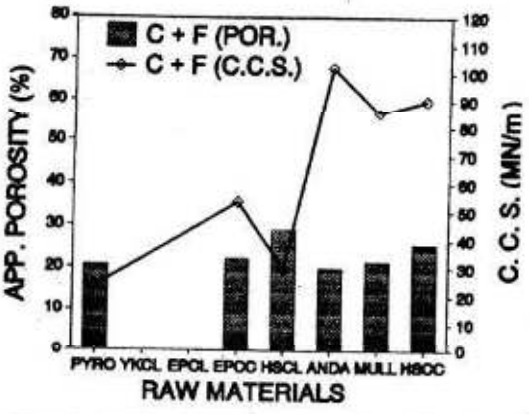

Fig 16a. A bar chart of apparent porosity and line plot of cold crushing strength for coarse-and-fine-grained bricks.

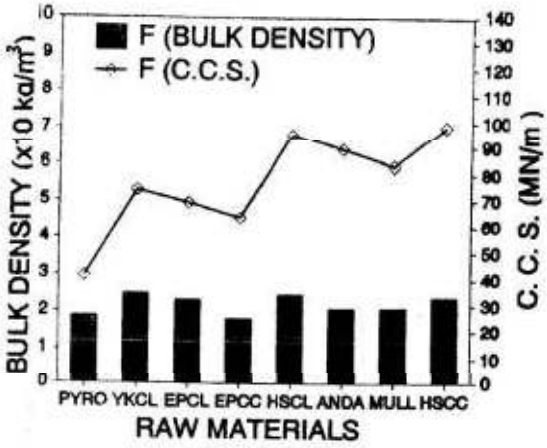

Fig 17a. A bar chart of bulk density and cold crushing strength (C.C.S.) for fine-grained bricks.

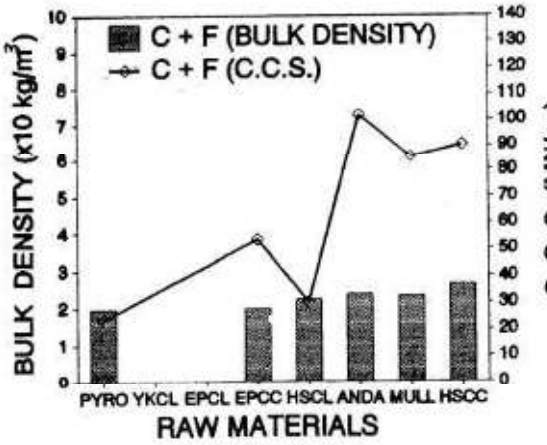

Fig 17b. A bar chart of bulk densities and cold crushing strength (C.C.S.) for coarse-and-fine-grained bricks.

parameters including porosity, the hardness of the grains, the bulk density and alumina content.

Refractoriness

Fig 18 shows a clear picture of refractoriness increasing with the Al_2O_3 content in the raw materials. It is a general practice for refractory manufacturers of high alumina bricks to improve the refractoriness of the bricks by incorporating raw materials with high alumina content, e g alumina, synthetic mullite, hard shale clay chamotte, sillimanite and andalusite.

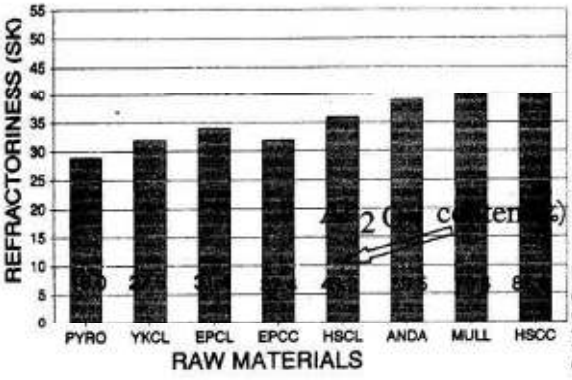

Fig 18. A bar chart of refractoriness of the raw materials.

CONCLUSION

A very important aspect in the manufacturing of refractories is to characterize the raw materials i.e. to test for the physical, thermal and mechanical properties of bricks made of single raw materials. The raw materials considered were grouped into the clay and non-clay types. The general conclusions are:

1. The clay materials - Yakusa Kibushi (Ball) Clay, Elutriated Plastic Clay and Hard Shale Clay went through large shrinkages and weight losses after firing.
2. The calcined clay (chamotte) had less volume shrinkage and weight loss. They are therefore added to bricks to improve on dimensional tolerance.
3. The coarse-and-fine-grained bricks of the non-clay materials, in general, had larger volume shrinkages than their corresponding fine-grained bricks.
4. The porosity values of the coarse-and-fine-grained bricks were lower than those of fine-grained bricks.
5. Apparent densities of the bricks were higher than their bulk densities.
6. For the non-clay materials, the bulk densities of the coarse-and-fine-grained bricks were higher than those of the fine-grained bricks.
7. For the clay materials, the C.C.S. values of fine-grained bricks were larger than those of the corresponding coarse-and-fine-grained bricks. The reverse trend was observed for the non-clay bricks.
8. The C.C.S. values were found to be dependent on the bulk density, the porosity, the alumina content of the raw materials and the grain size distribution.
9. The refractoriness of the raw material increased with the alumina content.

ACKNOWLEDGEMENTS

The author is grateful to the Japanese Government for providing funds which made it possible for this work to be carried out at Mino Yogyo Co. Ltd., a refractory manufacturing company in Japan. The author is also thankful to the entire management and staff of the company for their technical assistance. The efforts of the technical coordinator of the programme, Mr. T. Nabeta is very much appreciated. The team support of other group members is gratefully acknowledged.

REFERENCES

1. **Somiya, S.** *et al 'Taikabutsu', Vol 21, pg 137, 1969; J.A Ceram. Soc. Abstr. Vol 54, 1970.*

2. **Chester, J.H.,** *'Refractories', 1st Edition, pg 263, 266-268,474. Reprinted by The Institute of Materials, London, 1993.*

3. **Worrall, W.E.,** *'Clays and Ceramic Raw Materials', 2nd Edition. pgs v,30-44, 208, Pub. Elsevier Applied Science Publishers, London, 1986.*

4. *Techno Japan, Vol. 24, No. 5, pg 80, May 1991.*

5. **Singer, F. and Singer, S.S.,** *'Industrial Ceramics', 1st Edition, pgs 79,83,94,277,342,347, Pub. Chapman & Hall Ltd., London, 1963.*

6. **Dadson, A.B.C.,** *'Characterization of High Alumina Refratory Bricks made from Clay and non-Clay materials' to be published in the Journal of the University of Science and Technology.*

7. *Test method for the Aparent Porosity, Water Absorption and Specific gravity of Refractory Bricks, Japanese Industrial Standard (JIS), R2205, 1979.*

8. **Gould, R.W.,** *in 'Characterization of Ceramics' Ed. J.B Wachtman,Jr. pg 39-87, Pub. Marcel Dekker Inc. N.Y., 1971.*

9. **Cullity,B.D.,** *'Elements of X-rays Diffraction', 2nd Edition, pg 421-446, Pub. Addision-Wesley Publishing Co. Inc.,1978.*

10. **Stern,B.E. and Lewis,D.** *'X-Rays', 1st Edition, pg 202-211, Pub. Pitman Publishing, London, 1971.*

11. **Klug, H.P. and Alexander, L.E.** *'X-ray Diffraction Procedures for Polycrystalline and Amorphous Materials, 2nd Edition. pg 271-418, Pub. John Wiley & Sons, N.Y., 1974.*

12. *Test Method for Cold Crushing Strenth of Refractory Bricks, Japanese Industrial Standard (JIS), R2206, 1979.*

13. *Test Method for Refractoriness of Refractory Bricks, Japanese Industrial Standard (JIS), R2204, 1979.*

14. *Techno Japan, Vol. 25, No. 4, pg 40, April 1992.*

15. **Kingery, W.D., Bowen, H.K. and Uhlmann, D.R.,** *'Introduction to Ceramics', 2nd Edition, pg 507, Pub. John Wiley & Sons, Inc., 1976.*

16. **Norton, F.H.,** *'Refractories', 4th Edition, pg 183, Pub. McGraw-Hill Book Company, N.Y., 1968.*